Pergamon

0301-9322(94)00057-3

Int. J. Multiphase Flow Vol. 21, No. 1, pp. 61–74, 1995

0301-9322/95 $9.50 + 0.00

EXPERIMENTAL INVESTIGATION OF FLOW REGIMES AND OSCILLATORY PHENOMENA OF CONDENSING STEAM IN A SINGLE VERTICAL ANNULAR PASSAGE

B. D. BOYER,[1] G. E. ROBINSON[2] and T. G. HUGHES[3]

[1]Brookhaven National Laboratory, P.O. Box 5000, Building 475B, Upton, NY 11973-5000, U.S.A.
[2]Department of Nuclear Engineering, The Pennsylvania State University, University Park, PA 16802, U.S.A.
[3]Applied Research Laboratory, The Pennsylvania State University, University Park, PA 16802, U.S.A.

(Received 20 September 1993; in revised form 15 July 1994)

Abstract—Steam condensing in vertical annular passages experiences regular flow and pressure oscillations. An experimental program with a counterflow condensing heat exchanger with flow visualization was designed to obtain the flow and pressure data along with photographic and video records of condensing steam in vertical upflow in annular passages. The experimental results were compared to the literature on condensation oscillations.

From the observations and data collected in the experiment, a 3-region physical model of the condensing process was developed. This model contained a region of condensing annular flow, an interfacial region of slug and bubble flow, and a region containing subcooled condensate. It had been expected to find test conditions that would yield a stable condensing flow. However, flow and pressure oscillations were observed at all test conditions. While these oscillations were not particularly regular and sinusoidal, spectral analysis of the data revealed a 2–2.5 Hz oscillatory frequency. The observed flow and pressure oscillations were indicative of oscillations unique to condensing passages previously observed in condensation experiments that used a refrigerant as the working fluid.

Key Words: two-phase flow, condensation, flow oscillations, flooding

INTRODUCTION

The condensation process occurs when saturated vapor loses heat to a cooler surface, such as occurs in steam-filled tubes surrounded by a liquid coolant. This coolant serves as a heat sink causing the steam to condense on the tube surfaces. In vertical upflow the shear and liquid momentum forces on the condensate are small compared to the gravity forces. Hence, the condensate will flow down the inside of a cooled tube passage in a gravity-driven flow. In this situation, when saturated liquid forms on the cooled passage wall, gravity pulls the liquid down to the bottom of the passage. In a level passage or a passage with a downward inclination, the flowing vapor drives the liquid downstream along the passage. In a passage with an upward inclination, the magnitude of the vapor shear and downstream liquid momentum relative to the hydrostatic head of the condensate determines the ultimate direction of the liquid flow. If the condensate flows upward against gravity the flow is a shear-driven flow.

Several previous studies have dealt with oscillatory condensing flows and the relation between the forces of gravity and vapor shear, but they used refrigerants such as Refrigerant-12 as the working fluid. While working on a condenser for space applications, Soliman & Berenson (1970) investigated flow patterns, stability, and gravitational effects in condenser tubes of various geometries. They observed that the instabilities in a single condenser tube resulted from both gravity-dependent and gravity-independent instabilities. Liquid film runback and interface instabilities constituted the gravity-dependent instabilities. Wave trains observed on the surface of the liquid film created the gravity-independent instabilities. Bhatt (Bhatt 1978; Bhatt & Wedekind 1980; Bhatt *et al.* 1989) studied self-sustained condensing oscillatory flows of Regriferant-12 at high pressure in a horizontal tube. In these studies, the working fluid condensed from 100 to 0% quality. Starting with the mass and energy equations, Bhatt developed a model to predict the limit-cycle oscillations observed in the condenser. Bhatt (Bhatt 1978; Bhatt & Wedekind 1980) described the

condensing system as having 3 distinct regions: (1) an upstream vapor region, (2) a 2-phase condensing region, and (3) a downstream subcooled region. The energy storage mechanisms for the limit cycle were the upstream compressible vapor volume and downstream inertia. Bhatt also predicted the stability boundary of the occurrence of the oscillatory behavior.

The present research attempted to study the complete condensation of steam in a single annular passage of constant flow area in vertical upflow to study the stability of the condensing flows. The relationship between the gravity and shear forces in condensing steam flow in a vertically-inclined annular passage was studied qualitatively and quantitatively in this experiment. The transition point from a stable shear-driven flow to a gravity-driven flow was sought so that oscillatory flows could be predicted and avoided in a condenser. However, this experiment revealed that oscillatory flows will occur in all the flow conditions explored in this research. The observed oscillatory behavior was analyzed and compared to literature descriptions of various oscillatory mechanisms (Yadigaroglu & Bergles 1972; Yüncü 1990).

With the above background in mind, an experimental program with a condenser with flow visualization capabilities was designed to obtain the pressure and flow data along with photographic and video records needed (1) to examine condensing steam in vertical upflow, (2) to study and record the flow regimes and flow structures of condensing steam in vertical upflow, (3) to study and record the oscillatory nature of condensing steam in vertical upflow, and (4) to develop a simple physical model describing condensing flow behavior (Moore 1987; Piacsek 1991; Boyer 1992).

The experimental program addressed a matrix of coolant flow rates and steam-condensate flow rates as defined in figure 1. The first descriptive term denotes the coolant flow rate and the second descriptive term denotes the steam-condensate interface position for a specific test case. The designations low, medium, and high coolant for the coolant flows refer to 3 distinct coolant flow rates. However, the designations low, medium, and high steam for the steam flows refer to the bottom 1/4 of the tube, center of the tube, and top 1/4 of the tube positions of the vapor–liquid interface, respectively, instead of 3 distinct steam flow rates. All the tables in this study use these abbreviations to identify the experimental condensing conditions.

EXPERIMENTAL APPARATUS

The experimental apparatus, schematically shown in figures 2 and 3, is a counterflow heat exchanger with two annular passages configured in a counterflow fashion. An annular coolant passage was chosen over a circular coolant passage to provide optimal heat transfer. Subcooled water in the inner annulus cooled and condensed the steam in the outer annulus, as illustrated in figure 2. The condenser, constructed of aluminum, had the outer passage sealed with a clear viewing tube made of Plexiglas that slipped over the whole assembly. The condenser had a length of 89 cm with the outer and inner diameters of the condensing passage being 80.0 and 74.9 mm, respectively, creating a flow passage with a gap of 2.54 mm. The outer and inner diameters of the cooling passage were 69.9 and 74.9 mm, respectively, creating a flow passage with a gap of 2.54 mm. The tube wall

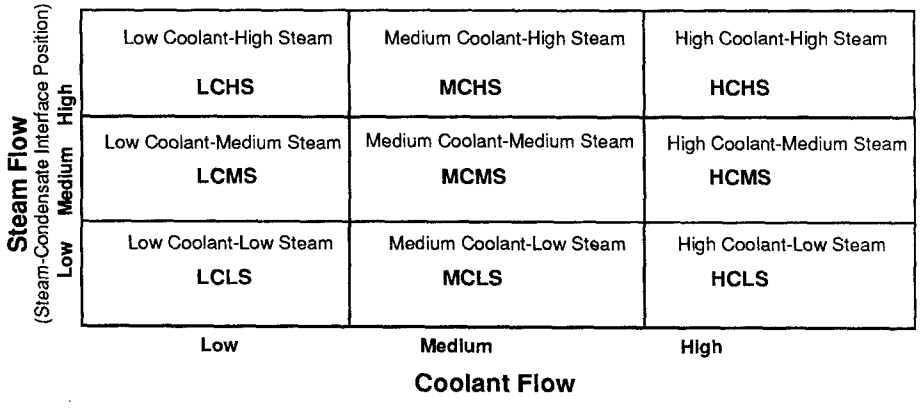

Figure 1. Flow visualization condensation test matrix.

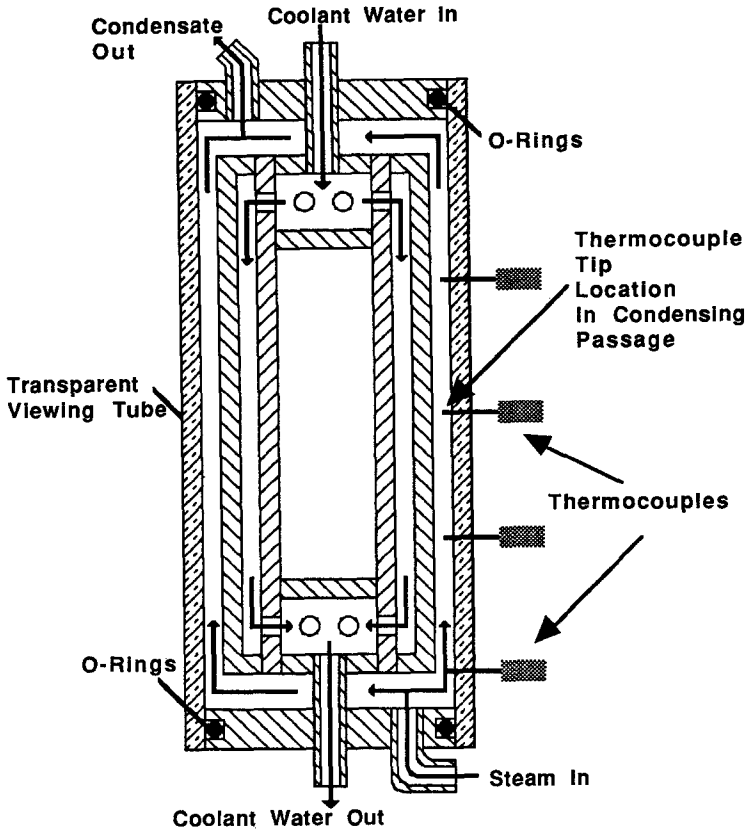

Figure 2. Cutaway schematic of flow visualization condenser.

thickness between the condensing and cooling passages was 2.54 mm. By varying the coolant and steam flow rates, the flow regimes and oscillatory phenomena in vertical upflow condensation in annular passages were explored.

With reference to figure 3, the experimental apparatus operated in the following manner. A set of circulation pumps supplied coolant water from a 114,000 liter water tank to the condenser through valves controlling coolant flow. Coolant entered the condenser through the top endfitting and flowed through the inner annulus cooling the steam. The coolant then exited through the bottom endfitting and drained back into the coolant tank that also served as the condenser heat sink. The large mass of coolant water in the coolant tank kept the rise in the coolant temperature to a maximum of 1–3°C during a normal experimental session. Under normal operating conditions, the coolant had a temperature ranging from 27 to 32°C at the condenser inlet. A set of circulation pumps produced a maximum flow rate of nearly 1.4 kg/s. In the course of passing through the test section, the coolant temperature rose about 8–17°C, depending on the test conditions, from the heat transfer from the steam.

A large boiler produced saturated steam at slightly above atmospheric pressure at temperatures of around 105–120°C depending on the flow conditions. The steam flowed through a series of control valves to a steam separator just upstream of the condenser. After leaving the steam separator, the saturated steam at a pressure of 120 kPa absolute to 150 kPa absolute flowed into the condenser inlet manifold. The inlet manifold attempted to distribute the steam in a radially symmetric fashion through a plate with 30 small circular holes. The steam then streamed up the annular passage, condensing on the aluminum coolant jacket. All of the condensate exited the tube as a slightly subcooled liquid through the outlet manifold. A pressure drop of less than 34 kPa existed across the condensing side. The condensate then flowed through piping containing a jewel-bearing flowmeter (FM # 1 on figure 1) sensitive enough to measure extremely low velocity liquid flows. Finally, the condensate entered the constant head producing device. The constant head producing device maintained a steady liquid head at the outlet. The constant head producing device

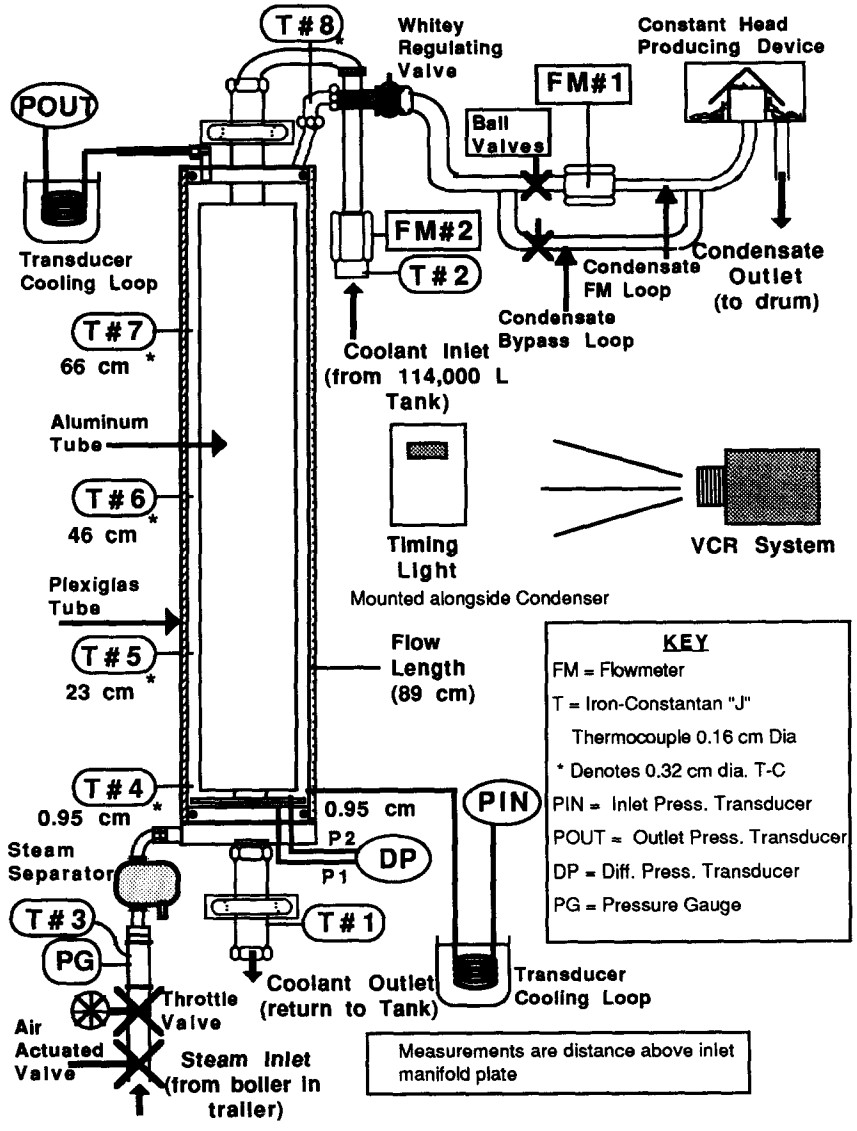

Figure 3. Flow visualization condenser experimental apparatus and instrumentation.

was about 30 cm higher than the outlet of the condenser to allow for making the weight calibration measurement. Hence, about 3 kPa of manifold pressure drop resulted from the head loss from elevation of the constant head producing device. The condensate exited the constant head producing device at atmospheric pressure to be funneled into a measuring bucket on a scale to measure an accurate time-averaged flow rate for the experiment.

INSTRUMENTATION

The instrumentation in this experiment was chosen to obtain heat transfer and flow data to quantify the visual observations of the oscillating flows. Eight iron–constantan thermocouples were inserted into the flow passages of the condenser as shown in figure 3. Since the thermocouple tips were located in the flow passages, the thermocouples recorded bulk temperatures. Thermocouples T # 1 and T # 2 recorded the coolant outlet and inlet temperatures, respectively. The other 6 thermocouples recorded the condensing passage temperatures with T # 3 measuring the inlet steam temperature, T # 4, T # 5, T # 6, and T # 7 measuring the steam–condensate mixture along the length of the condensing passage, and T # 8 measuring the temperature of the condensate in the

outlet piping approx. 15 cm above the exit. These thermocouples had a time constant of 1 s and had an accuracy of approx. $\pm 1°C$. Therefore, since the observed flow oscillations were much too rapid for the thermocouples to record changes in temperature accurately, the temperatures measured and reported in this paper are the average temperatures over the length of an experimental run.

Absolute pressure transducers (PIN and POUT on figure 1) were used to measure the inlet and outlet pressures on the condensing side of the apparatus. The pressure transducers were calibrated to an accuracy of $\pm 1\%$ over the range of operation. A ΔP pressure transducer was used to measure the pressure drop across the inlet manifold. Combining this pressure drop with a measurement of the loss factor across the inlet manifold allowed for the calculation of the inlet steam flow rate. The ΔP pressure transducer (0–69 kPa range) had a manufacturer's accuracy of $\pm 0.05\%$ full range of operation and was calibrated to an accuracy of $\pm 18\%$ at the lower range of operation and $\pm 5\%$ at the higher range of operation.

The coolant flowmeter (FM # 2 on figure 1) was a standard turbine flowmeter calibrated to an accuracy of $\pm 2\%$ over the range of operation. The flowmeter (FM # 1 on figure 1) used to measure the condensate flow was a paddlewheel jewel bearing flowmeter with modulated carrier pickoff accurate to low flow rates. This flowmeter had a 10 ms or better response to change of flow rate for a liquid working fluid. The low flow rates encountered in this experiment accentuated the inherent nonlinearity of this flowmeter. Hence, the flowmeter was calibrated to an accuracy of $\pm 20\%$ in the range of operation.

EXPERIMENTAL RESULTS

The experimental matrix for the flow visualization condensation experiment was run 6 times providing 6 sets of data for each of the 9 conditions listed in the matrix. Limits on the available coolant flow rates constrained the coolant and steam flow rates to the values chosen for the experimental matrix. For a specific experimental measurement in each of the 9 conditions, the data in all 6 sets showed only statistical scatter of about $\pm 10\%$ from the mean value. Since this lack of scatter indicated acceptable reproducibility of results, only the average value from all 6 cases will be shown in the tables and graphs of the 9 matrix conditions referenced in this section. Table 1, figures 4 and 5 contain summaries of the experimental data. The photos, videos, and experimental observations revealed the qualitative nature of the condensation process.

Table 1 shows the flow rate, pressure, and pressure drop data. Table 1 also presents the average interface positions observed in the experiment. Figures 6 and 7, photographs of the experiment, illustrate the actual oscillating interface. Figure 8, a sketch of the condensation process, defines where the interface would be at a particular instant. The average interface position is the average spot where the interface appeared during a review of the videotape of the tests. Table 2 presents all of the average thermocouple data. Figure 3 presents the average thermocouple data for the tube length and indicates the location of the interface between the vapor and liquid. Figure 4 presents the condensate subcooling along the tube length and indicates the location of the interface between the vapor and liquid.

Table 1. Summary of flow visualization condensing experiment flow and pressure data

Test titles	Coolant flow [FM # 2] (kg/s)	Average tube position steam–liquid interface (cm)	Condensate flow [WC] (kg/s)	Inlet pressure [PIN] (kPa)	Outlet pressure [POUT] (kPa)	Manifold pressure drop [DP] (kPa)	Tube ΔP (kPa)	Tube 2-phase ΔP (kPa)	Tube static head (kPa)	Outlet ΔP (kPa)	Total ΔP (kPa)
LCLS	0.77	23	0.011	119	112	4.1	9	2.8	6.2	8.3	21
LCMS	0.77	46	0.017	118	114	9.7	6.2	1.4	4.1	10	26
LCHS	0.77	66	0.021	119	116	17	5.5	3.4	2.1	12	34
MCLS	0.95	23	0.012	122	112	4.5	11	4.8	6.2	8.3	24
MCMS	0.95	46	0.019	122	114	12	9	4.8	4.1	11	32
MCHS	0.95	66	0.024	123	117	21	8.3	6.2	2.1	13	41
HCLS	1.2	23	0.012	122	112	4.8	12	4.8	6.2	8.3	25
HCMS	1.2	46	0.020	123	115	14	9	4.8	4.1	12	34
HCHS	1.2	66	0.026	125	118	26	8.3	6.2	2.1	14	48

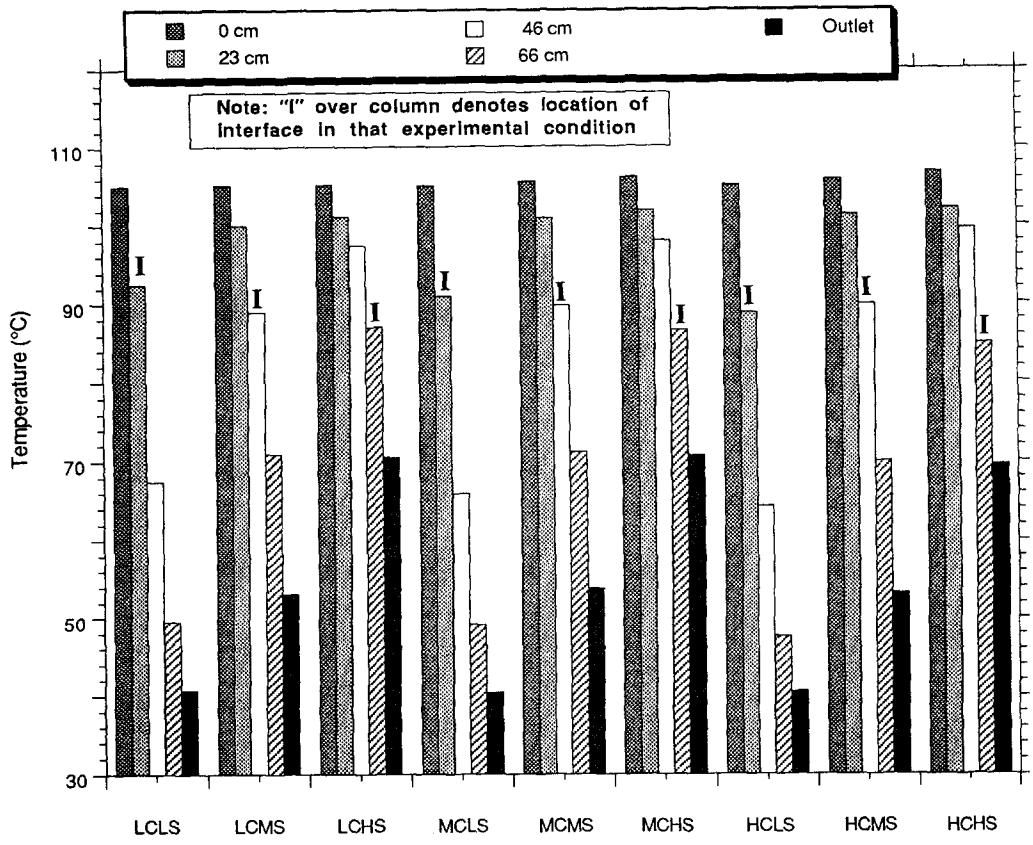

Figure 4. Steam–condensate temperatures along tube length.

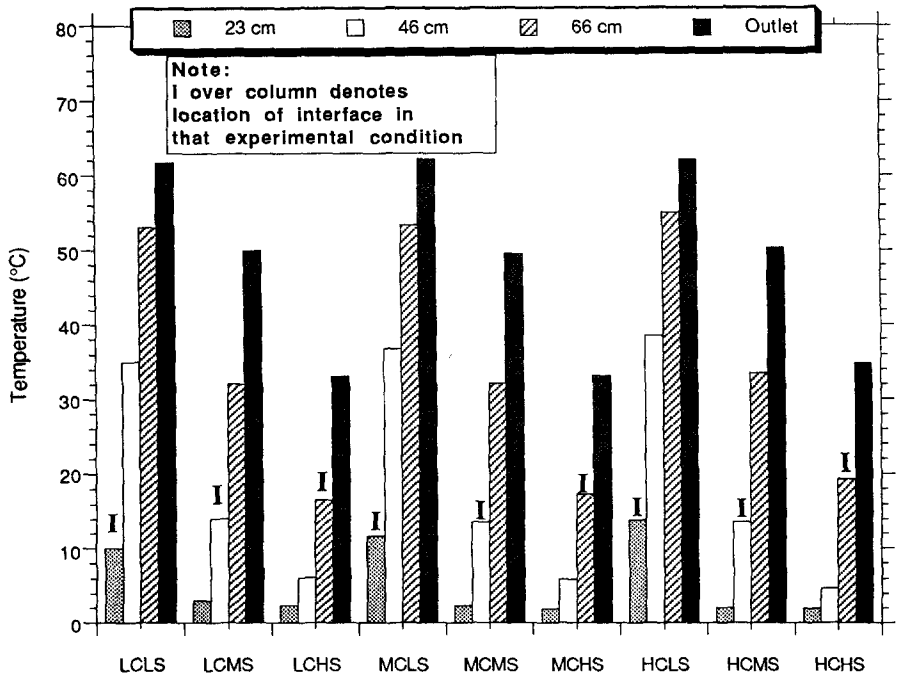

Figure 5. Condensate subcooling along tube length.

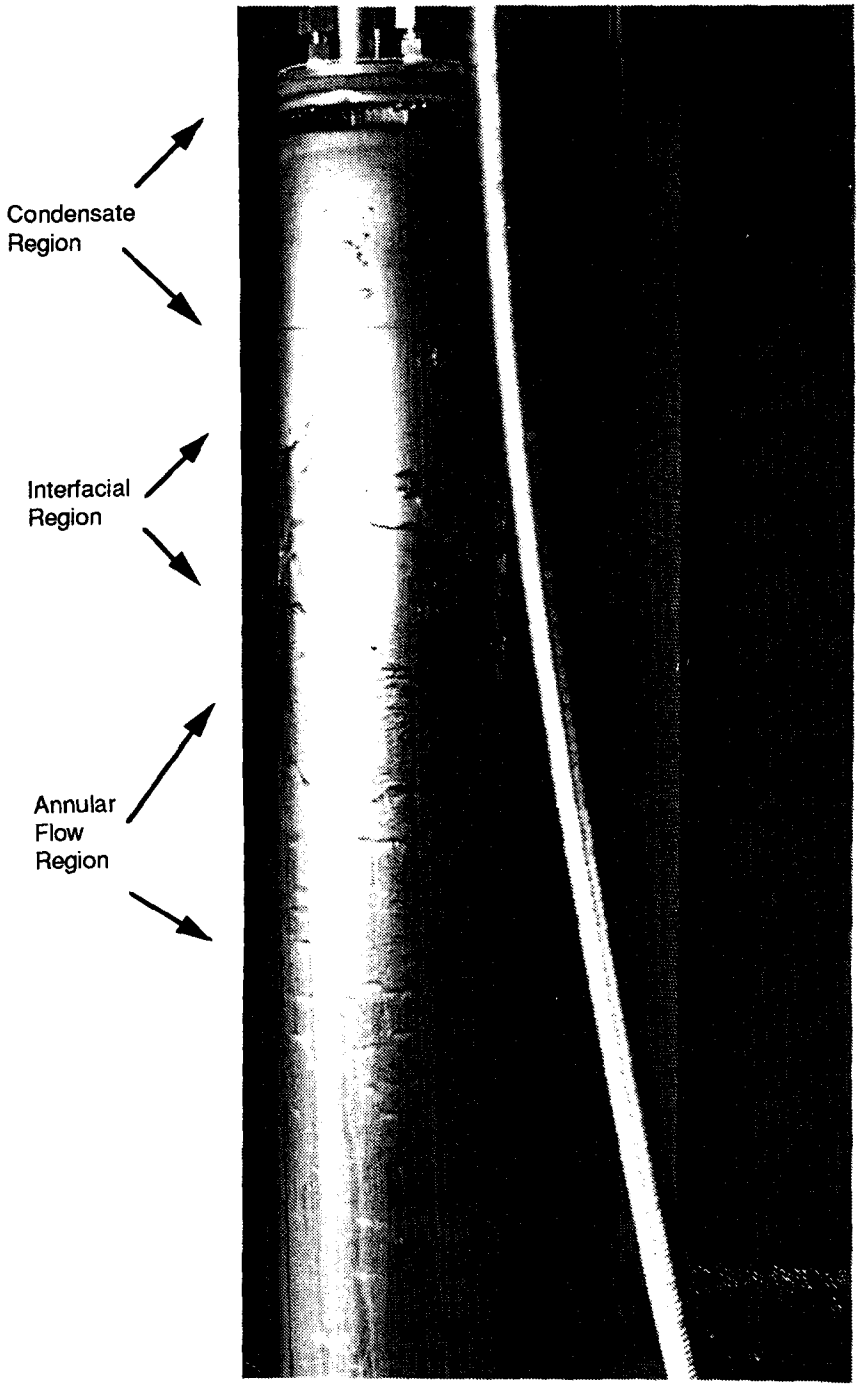

Figure 6. Condensing experiment illustrating flow structures and three region model of condensing.

The inlet and outlet flow rates and the pressures oscillated in all experimental cases. There were no cases where a stable condensing flow was observed quantitatively in the recorded data or qualitatively in the videotapes of the experiment. The time-series plots of inlet and outlet flow behavior and inlet and outlet pressure behavior, figures 9 and 10, provide a graphic snapshot of the oscillatory behavior observed in the flow visualization condenser tests. These plots are 5-s strips of the high coolant flow rate–high steam flow rate conditions that come from the sixth experimental series of the flow visualization condensation tests. The data in all 6 high coolant flow rate–high steam flow rate tests exhibited similar behavior. This oscillatory behavior was also seen in the other 8 experimental test matrix conditions of figure 1 in all 6 test series. The experimental standard

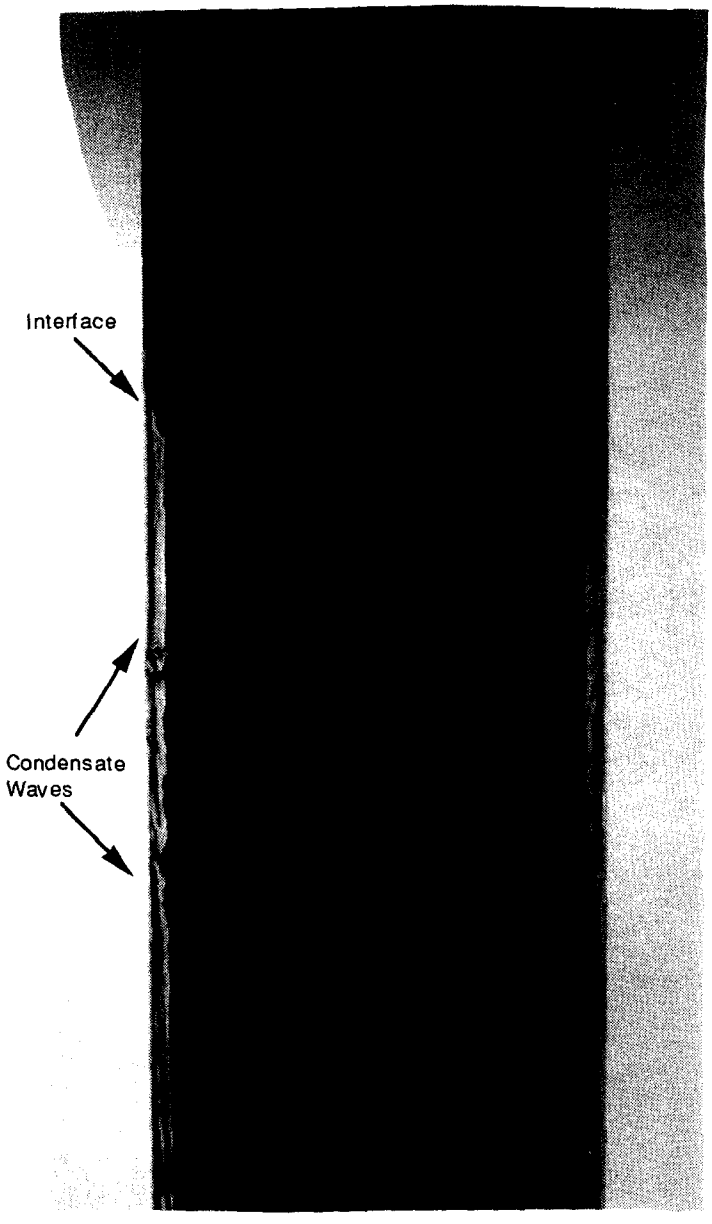

Figure 7. Condensing experiment vapor/liquid interface illustrating condensate waves moving up tube.

deviations, seen in table 3, can be assumed to be roughly equal to the amplitude of the oscillations. The videos of the experiment revealed that the steam–condensate interface had an oscillatory amplitude of approx. 7–8 cm. Furthermore, the time-series graphs show that the steam flows oscillated at a frequency of about 5–10 Hz in contrast to a frequency of 1–3 Hz that the time-series graphs show for condensate flow, inlet pressure, and outlet pressure. While the condensate flow rate, inlet pressure, and outlet pressure did not show a discernible relationship between flow rate and amplitude size, the inlet steam flow amplitude appeared inversely proportional to the inlet steam flow rate.

The video recordings and still photographs of the flow visualization condensation experiment captured the qualitative nature of condensation of vertically upflowing steam in an annular passage. From the videos and photographs, a predictable set of flow regimes in three regions characterized this condensation process. As shown in figures 6 and 8, the condensation of steam in vertical upflow has 3 regions identified as (1) the annular flow region containing steam condensing into liquid on the tube surface in annular two-phase flow, (2) the interfacial region containing two-phase flow

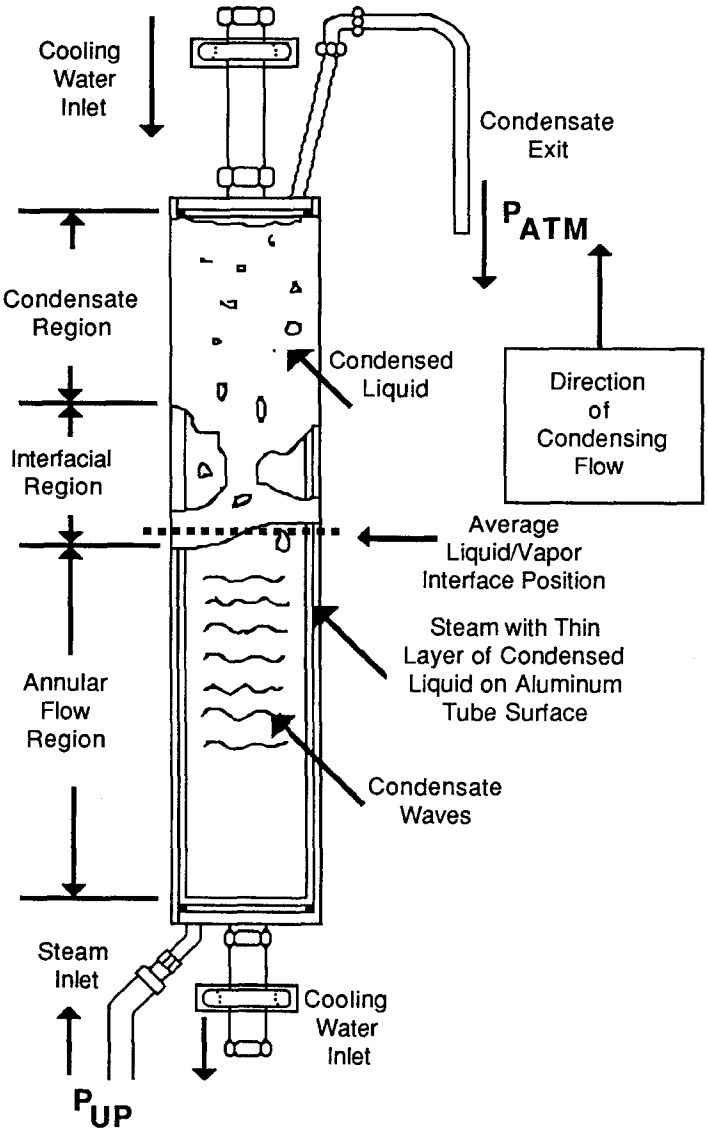

Figure 8. Three-region conceptual model of condensing.

consisting of swirling condensate slugs and steam bubbles in a slug flow regime, and (3) the condensate region containing subcooled liquid with a few collapsing and condensing steam bubbles.

The annular flow region had a swiftly moving vapor condensing in a slowly moving film on the heat transfer surface, annular flow regime characteristics, and prominent condensate waves forming

Table 2. Summary of flow visualization condensation experiment temperature data

Test titles	TC # 1 (°C)	TC # 2 (°C)	TC # 3 (°C)	TC # 4 (°C)	TC # 5 (°C)	TC # 6 (°C)	TC # 7 (°C)	TC # 8 (°C)	Coolant side ΔT (°C)	Tube saturation temperature (°C)
LCLS	41	31	108	105	93	68	50	41	9	103
LCMS	45	31	112	106	100	89	71	53	14	103
LCHS	48	31	116	106	101	98	87	71	17	104
MCLS	40	32	108	105	91	66	50	41	8	103
MCMS	44	32	113	106	101	90	71	54	12	103
MCHS	47	32	118	106	102	98	87	71	16	104
HCLS	39	32	108	105	89	65	48	41	7	103
HCMS	43	32	115	106	102	90	70	53	11	103
HCHS	46	32	121	107	102	100	85	70	14	104

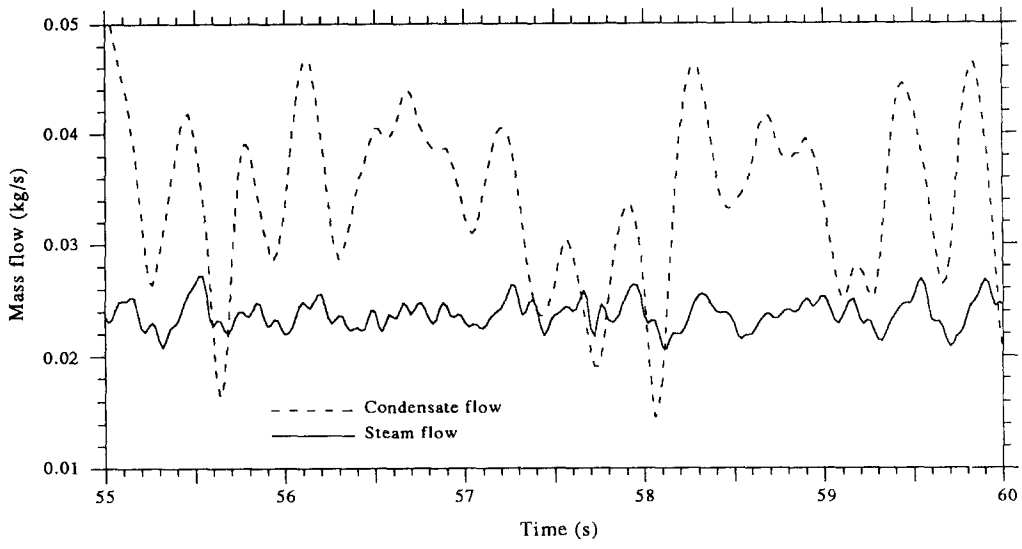

Figure 9. Run 6—high coolant–high steam flow rates.

and growing downsteam. As the condensate waves grew, the annular flow regime changed into a slug and bubble flow regime. This transformation defined the border between the annular flow and the interfacial region.

As shown in the photograph in figure 7, twisting and swirling steam and liquid eddies with slug and bubble flow regime characteristics defined the interfacial region. These eddies were approx. 8–10 cm in length and created loud audible cracking sounds as waves of condensed liquid crashed against the vapor–liquid interface and the condensing steam bubbles collapsed (Piacsek 1991; Boyer 1992). An examination of the videotape of the experiment showed that the vapor–liquid interface oscillated with an amplitude of ~8 cm. The point where the swirling interface with its two-phase slug flow turns into a single-phase flow with a few steam bubbles and minimal circumferential swirling defines the border between the interfacial and condensate regions.

The condensate region had a slowly moving subcooled liquid mixed in with a few collapsing and condensing steam bubbles. The recorded temperatures show that the bulk temperature of this region was subcooled. The videos showed that the steam bubbles were at most 1–2% steam by

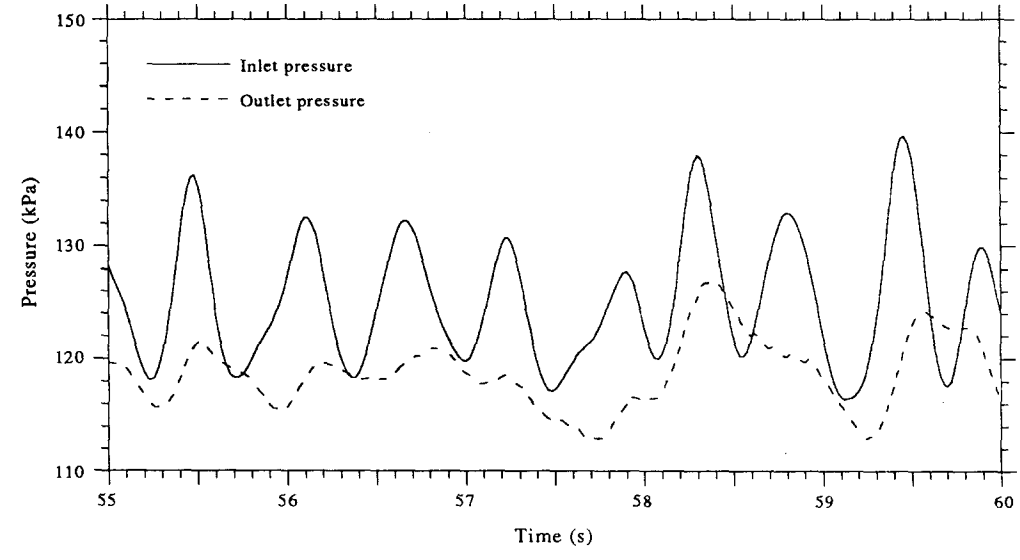

Figure 10. Run 6—high coolant–high steam pressures.

Table 3. Flow visualization condensing experiment—standard deviations of flow rates and absolute pressures

Test titles	Steam flow [STM (DP)] (g/s)	Condensate flow [FM # 1] (g/s)	Inlet pressure [PIN] (kPa)	Outlet pressure [POUT] (kPa)
LCLS	2.1	5.5	3.4	2.8
LCMS	1.5	6.4	3.9	3.2
LCHS	1.3	7.7	4.2	3.4
MCLS	2.2	5.5	3.7	2.8
MCMS	1.5	7.3	4.6	3.5
MCHS	1.3	7.7	4.7	3.5
HCLS	2.2	5.9	3.8	3
HCMS	1.5	7.3	4.8	3.7
HCHS	1.4	7.7	5.2	3.7

volume. Therefore, the condensate region had an essentially single-phase liquid flow. Because of the large change in density from steam to liquid, the velocity of the liquid flow was considerably lower than the velocity of the steam flow.

The physical model described the flow and pressure oscillations that occur in the following manner. The model assumed the pressure P_{UP}, the upstream steam pressure, and P_{ATM}, the outlet atmospheric pressure, shown in figure 8, will remain constant. As the condensate outflow increased, the interface moved up the tube uncovering the inner annulus. This interface displacement increased heat transfer surface area. The inlet pressure decreased as the lower density steam displaced the higher density liquid as the interface rose. With increased heat transfer area, the condensation rate increased acting to increase the condensate at the interface thus causing the interface to move down the tube. With decreased inlet pressure, the pressure drop across the inlet manifold increased causing an increase in the steam flow. As the inlet pressure decreased, the outlet condensate flow rate began to drop. Therefore, the outlet flow rate and the interface position dropped while the inlet steam flow increased. The dropping interface covered the inner annulus reducing the heat transfer surface area, which reduced the condensation rate and increased the inlet pressure. As the inlet pressure built up, the inlet steam flow decreased and the tube pressure drop increased. The increased tube pressure drop caused the condensate outflow to increase starting the cycle again. This is the self-sustained oscillatory cycle shown in the photos and in the time-series graphs.

Furthermore, the videos and the stills also captured the waves on the liquid film and the gravity-dependent instabilities seen by Soliman & Berenson (1970). The photographs of the condensing flow (figures 6 and 7) reveal waves on the liquid condensate film forming and growing as the condensate film moved up the tube. When they grew large enough to bridge the tube annulus (figures 7 and 8), the annular flowing steam and condensate mixture transformed into a slug and plug flowing mixture as shown in the interfacial region in figure 6. Gravity-dependent instabilities such as liquid film runback and interface instability, occurred in this swirling and churning interface. As was seen in the plots of figures 9 and 10 and table 3, the videos and the photos show that the liquid film runs back but does not totally "plug" the tube or create extremely violent oscillations. The unstable meniscus of condensate at the steam–condensate interface characterized the interface instability. This meniscus appeared to be unstable, both vertically and circumferentially. The steam and liquid interface swirled horizontally in 3–6 cm eddies that caused the interface to vary vertically from 3 to 8 cm as shown in the photo in figure 6 and the sketch in figure 8. This pronounced circumferential motion was evident even after inserting several different inlet manifolds designed to better distribute the inlet steam evenly around the circumference of the inlet manifold plate. Therefore, as the average location of the interface moved 7–8 cm up and down the tube, some portions of the interface moved 2–3 cm and some portions of the interface moved 7–9 cm.

The thermocouple data had the interesting and rather unexpected result that the temperature at the vapor–liquid interface shown in figures 7, 8, and 9 suggests substantial subcooling (10–19°C) in the condensate at a location where the condensate should have been saturated, not subcooled. The subcooling at the interface was the difference between the temperature at the interface location and the saturation temperature. Figures 3 and 4 show how the subcooling at the interface increased as the steam flow rate increased. However, as the steam flow rate went down, the total subcooling at the outlet decreased. It should be noted that calculations revealed that subcooling of the

condensate constituted at most 10% of the total heat transfer occurring on the steam–condensate side. Condensation constituted the rest of the heat transfer. With the violent chugging and slugging leading to increased convective heat transfer in two-phase mixture, subcooling and condensing easily could have simultaneously occurred in the two-phase mixture prior to the point of total condensation. Since the condensing length increased with increasing steam rate, the mixing of steam and water increased and the subcooling increased. However, since the length of the liquid region above the condensing vapor decreased with increasing steam rate, the heat transfer area of the tube that existed for the subcooling of the condensed liquid decreased. Hence, this decrease in heat transfer area reduced the total subcooling in that test condition.

FREQUENCY ANALYSIS OF FLOW AND PRESSURE OSCILLATIONS

While behaving as a limit cycle, the data taken did not appear to have the highly sinusoidal limit cycle that Bhatt *et al.* (Bhatt 1978; Bhatt & Wedekind 1980; Bhatt *et al.* 1989) found in their condensation studies with Refrigerant-12 as the working fluid. Therefore, Fast Fourier Transforms (FFT) (Bendat & Piersol 1980) were used to analyze the spectral density of the experimental flows and pressures to locate an organized structure in the observed flow and pressure oscillations. Figures 11 and 12 are plots of the averages of the FFT plots of the steam and condensate flow rates and the inlet and outlet pressures from the 6 high coolant flow rate–high steam flow rate tests. These plots can be compared to the time-series plots of the same test conditions in figures 9 and 10. From these spectral plots, a break frequency can be defined as a point where the nearly flat horizontal line at the low frequencies intersects the downward sloping line of the higher frequencies (Schultz 1961). This frequency equals the inverse of the period of oscillation. The inverse of the period of oscillation is the oscillatory frequency. Therefore, the break frequency in the FFT plots is the frequency of the flow and pressure oscillations in the experimental runs (table 3).

As shown in figures 11 and 12, the steam and condensate flow rates and the inlet and outlet pressures exhibit approximately a distinct 40 dB/decade drop starting at the break frequency. Therefore, the spectral analysis indicates an ordered structure to the flow and pressure oscillations. This 40 dB/decade drop is representative of a second-order transfer function such as seen in a mass and spring suspension system (Boyer 1992; Schultz 1961).

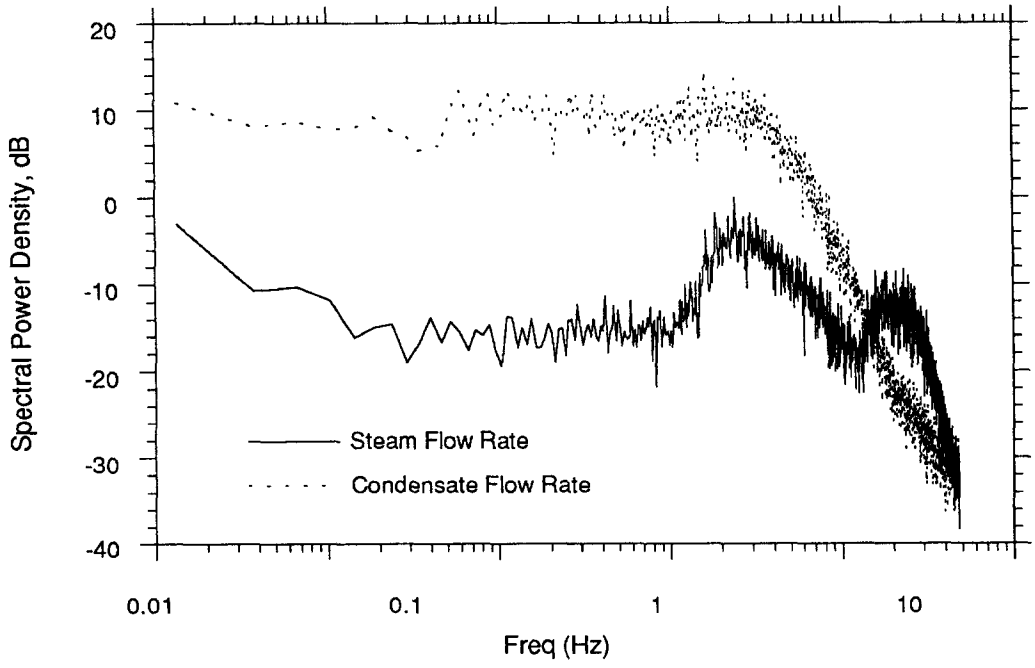

Figure 11. FFT of condensing experiment high coolant–high steam run flow rates.

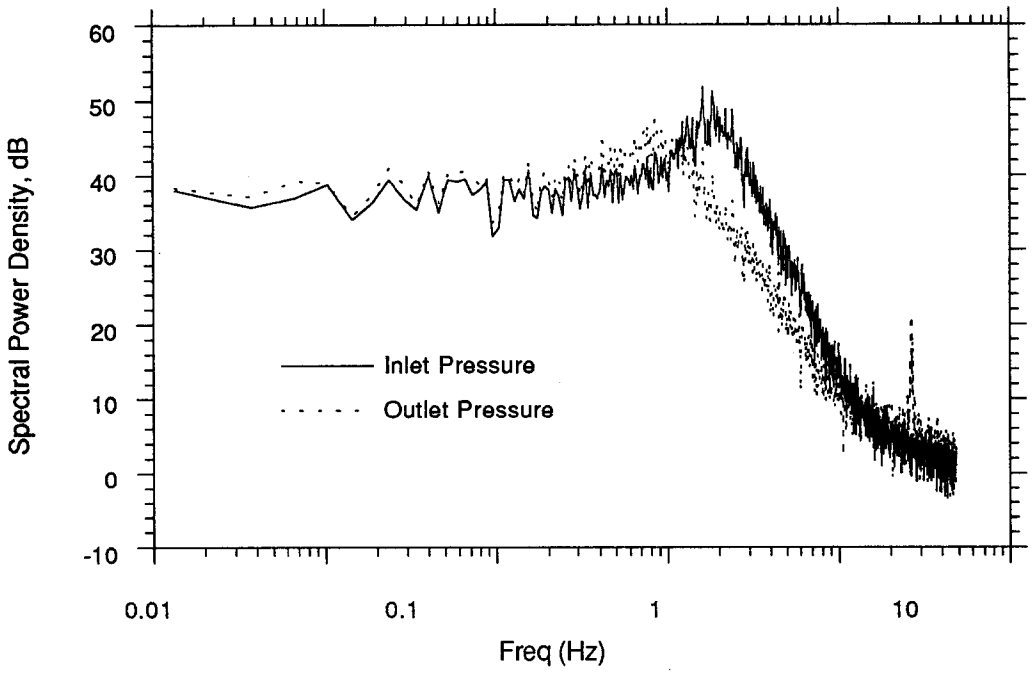

Figure 12. FFT of condensing experiment high coolant–high steam run pressures.

These break frequencies also showed the independence of the oscillations from the fluid transit time in the flow visualization condensation experiment. The uniform experimental break frequencies of 2–2.5 Hz correspond to oscillatory periods of less than 1 s. These periods were all lower than the transit times of the fluid estimated to range from 5 to 35 s (~35 s for low coolant flow rate–low steam flow rate tests dropping to ~5 s for high coolant flow rate–high steam flow rate tests). Furthermore, as the transit times dropped when the steam flow rate increased, the sharply decreasing fluid transit times did not appreciably affect the break frequencies. Density wave oscillations are dependent on and have a period of the same magnitude as the fluid transit times and have a positive sloping pressure drop versus flow curve (Bhatt *et al.* 1989; Boyer 1992; Yadigaroglu & Bergles 1972; Yüncü 1990). However, in the flow visualization condensation experiment, the independence from the fluid transit times and the higher magnitude of the fluid transit times compared to the oscillatory periods (~0.5 s) combined with the negative sloping pressure drop versus flow curve ruled out density waves as the oscillatory mechanism. Furthermore, since the oscillations had frequencies higher than expected for either density wave or especially pressure drop oscillations, the observed oscillations had the characteristics of condensation oscillations observed by Bhatt (Bhatt *et al.* 1989).

Bhatt (Bhatt *et al.* 1989) observed oscillations in a condensing system that occurred with a nearly flat pressure drop versus flow rate curve that had frequencies higher than expected for either density wave or pressure drop oscillations. While condensing system oscillation frequencies are strongly

Table 4. Flow visualization condensation experiment—estimated break frequencies

Test titles	Condensate flow (Hz)	Steam flow (Hz)	Inlet pressure (Hz)	Outlet pressure (Hz)
LCLS	2.0	6.5	1.5	0.9
LCMS	2.0	6.5	1.5	0.9
LCHS	2.0	7.0	1.5	0.9
MCLS	2.0	6.0	1.5	0.9
MCMS	2.0	7.0	1.5	0.9
MCHS	2.5	7.0	1.5	0.9
HCLS	2.0	6.5	1.5	0.9
HCMS	2.5	7.0	1.5	0.8
HCHS	2.5	7.0	1.5	0.9

dependent on the upstream vapor volume in the two-phase region of the condensing system, evaporating system oscillation frequencies are normally related to the fluid transport time through the evaporator. Bhatt believed the observed oscillatory phenomena to be unique to condensing systems. The present flow visualization condensation experiment also appears to contain this same type of oscillatory phenomenon unique to condensing systems.

CONCLUSIONS

This study examined flow regimes and oscillatory phenomena of condensing steam in a single vertical annular passage. From the earlier research it had been thought that steady condensing flows may be observed (Soliman & Berenson 1970; Bhatt 1978; Bhatt & Wedekind 1980; Bhatt *et al.* 1989), but there were no experimental cases observed that had a steady stable condensing flow. Therefore, steam condensation had more irregular flow and pressure oscillatory behavior than seen in the refrigerant condensation described heavily in the literature. While the flow and pressure oscillations in the present experiment were bounded but not particularly sinusoidal, spectral analysis revealed a 2–2.5 Hz oscillatory frequency. Furthermore the presence of these oscillations in all test conditions revealed that there were no regimes of smooth vapor-driven flow that disintegrated into a flow disrupting gravity-driven backflow. These flow and pressure oscillations were indicative of oscillations unique to condensing passages seen by Bhatt *et al.* (1989) and were shown by spectral analysis to be of a second order nature indicative of a spring and mass oscillatory system.

REFERENCES

BENDAT, J. S. & PIERSOL, A. G. 1980 *Engineering Applications of Correlation and Spectral Analysis.* Wiley–Interscience, New York.

BHATT, B. L. 1978 An experimental and theoretical study of various transient and oscillatory flow phenoneoma in two-phase condensing flow systems. Ph.D thesis, Oakland University, Rochester, Michigan.

BHATT, B. L. & WEDEKIND, G. L. 1980 A self-sustained oscillatory flow phenomenon in two-phase condensing flow systems. *Trans. ASME J. Heat Transfer* **105,** 694–700.

BHATT, B. L., WEDEKIND, G. L. & JUNG, K. 1989 Effects of two-phase pressure drop on the self-sustained oscillatory instability in two-phase condensing flows. *Trans. ASME J. Heat Transfer* **111,** 538–545.

BOURE, J. A., BERGLES, A. E. & TONG, L. S. 1973 Review of two-phase flow instability. *Nucl. Engng Design* **25,** 165–192.

BOYER, B. D. 1992 An investigation of flow regimes and oscillatory phenomena of condensing steam in a single vertical passage. Doctor of philosophy thesis, the Pennsylvania State University, University Park, PA.

MOORE, J. T. 1987 Development of the design of a working condenser with flow visualization capabilities. Master of Science Paper, the Pennsylvania State University, University Park, PA.

PIACSEK, A. A. 1991 A study of transient vibrations in condensing two-phase flow. Master of Science thesis, the Pennsylvania State University, University Park, PA.

SCHULTZ, M. A. 1961 *Control of Nuclear Reactors and Power Plants*, pp. 72–77. McGraw–Hill, New York.

SHEARER, J. L., MURPHY, A. T. & RICHARDSON, H. H. 1967 *Introduction to System Dynamics*, pp. 24–70. Addison–Wesley, Reading, MA.

SOLIMAN, M. & BERENSON, P. J. 1970 Flow stability and gravitational effects in condenser tubes. Paper No. Cs 1.8, *Proceedings of the Fourth International Heat Transfer Conference*, Paris, Vol. VI.

WALLIS, G. B. & MAKKENCHERY, S. 1974 The hanging film phenomenon in vertical annular two-phase flow. *ASME Trans. J. Fluids Engng* **96,** 297–298.

YADIGAROGLU, G. & BERGLES, A. E. 1972 Fundamental and higher-mode density-wave oscillations in two-phase flow. *Trans. ASME J. Heat Transfer* **94,** 189–195.

YÜNCÜ, T. 1990 An experimental and theoretical study of density wave and pressure drop oscillations. *Heat Transfer Engng* **11,** 45–56.